Check for updates

Host-Induced Gene Silencing of the MAPKK Gene *PsFUZ7* Confers Stable Resistance to Wheat Stripe Rust[1]

Xiaoguo Zhu,[a] Tuo Qi,[a] Qian Yang,[a] Fuxin He,[a] Chenglong Tan,[a] Wei Ma,[a] Ralf Thomas Voegele,[b] Zhensheng Kang,[a,2] and Jun Guo[a,2]

[a]State Key Laboratory of Crop Stress Biology for Arid Areas, College of Plant Protection, Northwest A&F University, Yangling 712100, Shaanxi, China

[b]Department of Phytopathology, Institute of Phytomedicine, Faculty of Agricultural Sciences, University of Hohenheim, 70599 Stuttgart, Germany

ORCID IDs: 0000-0002-6068-8244 (R.T.V.); 0000-0002-5552-734X (J.G.).

RNA interference (RNAi) is a powerful genetic tool to accelerate research in plant biotechnology and control biotic stresses by manipulating target gene expression. However, the potential of RNAi in wheat to efficiently and durably control the devastating stripe rust fungus *Puccinia striiformis* f. sp. *tritici* (*Pst*) remained largely under explored so far. To address this issue, we generated transgenic wheat (*Triticum aestivum*) lines expressing dsRNA targeting *PsFUZ7* transcripts of *Pst*. We analyzed expression of *PsFUZ7* and related genes, and resistance traits of the transgenic wheat lines. We show that *PsFUZ7* is an important pathogenicity factor that regulates infection and development of *Pst*. A *PsFUZ7* RNAi construct stably expressed in two independent transgenic wheat lines confers strong resistance to *Pst*. *Pst* hyphal development is strongly restricted, and necrosis of plant cells in resistance responses was significantly induced. We conclude that trafficking of RNA molecules from wheat plants to *Pst* may lead to a complex molecular dialogue between wheat and the rust pathogen. Moreover, we confirm the RNAi-based crop protection approaches can be used, to our knowledge, as a novel control strategy against rust pathogens in wheat.

Global wheat (*Triticum aestivum*) yields are estimated to be reduced by 3% to greater than 90% per year because of the obligate biotrophic pathogen *Puccinia striiformis* f. sp. *tritici* (*Pst*), jeopardizing global food security (Wellings, 2011; Chen, 2014). It is evident that *Pst* constitutes a significant threat to wheat production worldwide. Currently, approaches to manage this disease rely on cultivar resistance coupled with fungicide application (Chen, 2014). However, driven by a greater need for wheat production (Singh et al., 2011), the necessity for environmental protection (Ishii, 2006), the constant evolution of virulence in rust fungi (Chen et al., 2009), and the loss of natural resistance in wheat cultivars (Mcintosh et al., 1995), innovative alternative approaches to control rust disease are urgently required. To date, several technologies have been used to transiently silence *Pst* genes to restrict pathogen development (Panwar et al., 2013; Fu et al., 2014). However, the pathogen is capable of overcoming this transient resistance barrier, and hence, strategies conferring durable resistance to *Pst* must be sought.

A powerful genetic tool, RNA interference (RNAi), a conserved eukaryotic mechanism that performs a crucial role in gene regulation, has been used to enhance crop resistance by silencing critical genes (Bartel, 2004; Baulcombe, 2004). A key conserved trait of RNAi is the cleavage of precursor double-stranded RNA (dsRNA) into short 21- to 24-nucleotide small interfering RNAs (siRNAs) by a RNase called "DICER", or "Dicer-like" (Fagard et al., 2000). siRNAs are then incorporated into the RNA-induced silencing complex containing an Argonaute protein (Fagard et al., 2000). Subsequently, specific degradation of the target mRNA sharing sequence similarity with the inducing dsRNA takes place (Ghildiyal and Zamore, 2009; Liu and Paroo, 2010). Numerous reports have demonstrated the efficiency of RNAi to improve control of bacteria, viruses, fungi, insects, nematodes, and parasitic weeds (Saurabh et al., 2014). Insects feeding on transgenic plants carrying RNAi constructs against genes of the pest were severely constrained in their development (Huang et al., 2006; Baum et al., 2007; Mao et al., 2007). In genetically engineered RNAi crop plants, defense against fungi

[1] This study was supported by the National Natural Science Foundation of China (grant nos. 31620103913 and 31371889), the National Basic Research Program of China (grant no. 2013CB127700), the 111 Project from the Ministry of Education of China (grant no. B07049), and Natural Science Basic Research Plan in Shaanxi Province of China (grant no. 2017JM3007).

[2] Address correspondence to guojunwgq@nwsuaf.edu.cn or kangzs@nwsuaf.edu.cn.

The authors responsible for distribution of materials integral to the findings presented in this article in accordance with the policy described in the Instructions for Authors (www.plantphysiol.org) are: Zhensheng Kang (kangzs@nwsuaf.edu.cn) and Jun Guo (guojunwgq@nwsuaf.edu.cn).

J.G. and Z.S.K. designed the experiments; X.G.Z., T.Q., Q.Y., F.X. H., C.L.T., and W.M. performed the experiments; X.G.Z., J.G., R.T.V., and Z.S.K. analyzed the data and wrote the article; all authors discussed the results and commented on the manuscript.

www.plantphysiol.org/cgi/doi/10.1104/pp.17.01223

 © 2017 American Society of Plant Biologists. All Rights Reserved.

was substantially enhanced (Nowara et al., 2010; Koch et al., 2013; Ghag et al., 2014). Host-induced gene silencing (HIGS) of the *Fusarium* cytochrome P450 lanosterol C-14α-demethylase gene, which is essential for ergosterol biosynthesis, confers resistance of barley (*Hordeum vulgare*) to *Fusarium* species (Koch et al., 2013). During interaction of the host with the pathogen *Blumeria graminis*, siRNA molecules are exchanged and restrict fungal development in plants carrying RNAi constructs targeting fungal transcripts (Nowara et al., 2010).

MAPK cascades regulate a variety of cellular processes in response to extracellular and intracellular stimuli (van Drogen and Peter, 2002). In our study, the MAPK kinase gene *PsFUZ7*, which was shown to play an important role in *Pst* virulence by regulating hyphal morphology and development, was selected as the target for RNAi. Our results indicate that the expression of RNAi constructs in transgenic wheat plants confers strong and durable resistance to *Pst*, along with a severe restriction of *Pst* development. This efficient inhibition of disease development suggests that HIGS is a powerful strategy to engineer transgenic wheat resistant against the obligate biotrophic pathogen *Pst* and has potential as an alternative approach to conventional breeding, or chemical treatment for the development of environmentally friendly and durable resistance in wheat and other food crops.

RESULTS

Three MAPK Cascade Genes Are Highly Induced during *Pst* Differentiation

During our search for potential genes that regulate the development of *Pst*, we identified and cloned five candidate genes from the virulent *Pst* strain CYR32. These genes were found to be orthologs of *Ustilago maydis* MAPK signaling pathway-related genes (Supplemental Table S1). Transcript profiles assayed by quantitative real-time PCR (qRT-PCR) show that *PsKPP4*, *PsFUZ7*, *PsKPP6*, and *PsCRK1* are all induced at early differentiation stages, whereas *PsKPP2* is significantly downregulated during this phase (Fig. 1). Transcript levels of *PsKPP4*, *PsFUZ7*, and *PsKPP6* are increased more than 30-fold during the very early stage of colonization of wheat by urediospores (12 h), and the time of primary haustorium formation (18 h), the stage indicating successful colonization of the host. *PsKPP4* and *PsFUZ7* are induced more than 20-fold during secondary hyphae formation (48 h to 72 h), the stage essential for hyphal expansion. These results suggest that *PsKPP4*, *PsFUZ7*, and *PsKPP6* participate in early *Pst* development. Therefore, these genes were chosen as target genes for subsequent virus-induced gene silencing (VIGS) experiments.

Transient Silencing of *PsFUZ7* Significantly Inhibits Growth of *Pst*

VIGS mediated by the barley stripe mosaic virus (BSMV) has been established in barley and wheat (Holzberg et al., 2002; Scofield et al., 2005). To confirm the effect of silencing *PsKPP4*, *PsFUZ7*, and *PsKPP6* during the interaction between wheat and *Pst* strain CYR32, two approximately 250-bp silencing sequences of each gene were derived from the 5′- and the 3′-prime end of the gene to generate different BSMV constructs (Supplemental Table S2), respectively. At 14 d postinoculation (dpi) with *Pst*, generation of uredia is suppressed in plants inoculated with BSMV-silencing sequences, and those carrying BSMV:*PsFUZ7*-as constructs show the highest inhibition of uredia formation (Fig. 2A). qRT-PCR analysis of total RNA isolated from silenced leaves sampled at 2 dpi and 7 dpi, revealed

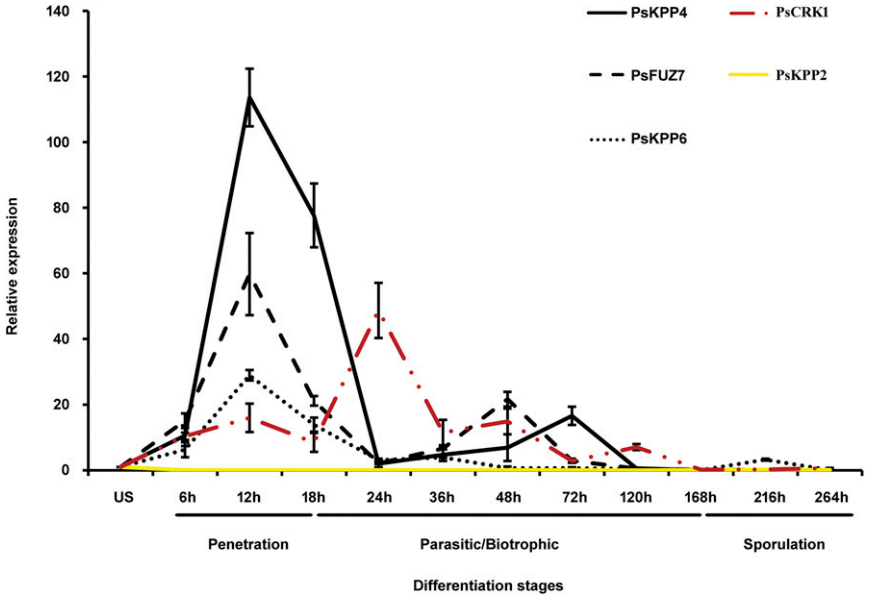

Figure 1. Transcript profiles of five MAPK cascade genes at different *Pst* infection stages. Wheat leaves (Su11) were inoculated with fresh urediospores (CYR32) and kept in the dark and under high humidity for 24 h. Inoculated leaves were sampled at different time points according to the differentiation stage of *Pst*. Gene expression levels were normalized to the expression level of *PsEF-1*. Results are expressed as means ± SE of three biological replicates. US, Urediospores; 6h to 264h, 6 h to 264 hpi with CYR32; *PsKPP4*, MAP kinase kinase kinase gene; *PsFUZ7*, MAP kinase kinase gene; *PsKPP2*, *PsKPP6*, and *PsCRK1*, MAP kinase genes.

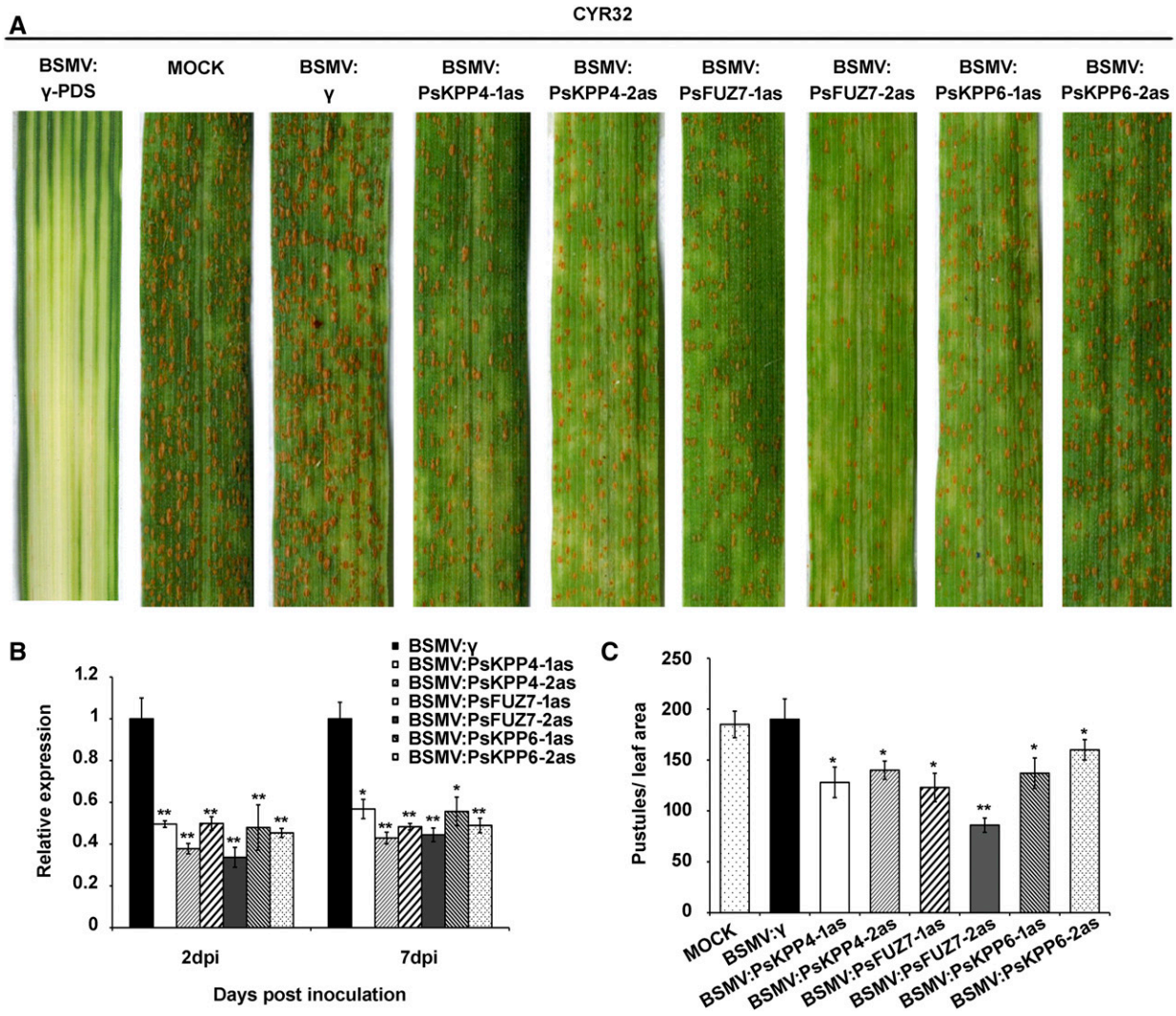

Figure 2. Functional assessment of *PsKPP4*, *PsFUZ7*, and *PsKPP6* in the wheat-*Pst* interaction by virus-induced gene silencing. A, Phenotypes of fourth leaves inoculated with CYR32 at 14 dpi. Plants were preinoculated with FES buffer (mock), BSMV:*TaPDS*, BSMV:γ, BSMV:*PsKPP4*-1as, BSMV:*PsKPP4*-2as, BSMV:*PsFUZ7*-1as, BSMV:*PsFUZ7*-2as, BSMV:*PsKPP6*-1as, or BSMV:*PsKPP6*-2as, respectively. B, Relative transcript levels of *PsKPP4*, *PsFUZ7*, and *PsKPP6* in knockdown plants inoculated with CYR32 at 2 and 7 dpi. Wheat leaves inoculated with BSMV:γ and sampled after inoculation with CYR32 were used as controls. Data were normalized to the transcript level of *PsEF-1*. Asterisks indicate $P < 0.05$; double asterisks indicate $P < 0.01$. C, Quantification of uredial density in silenced plants 14 dpi with CYR32. Differences were assessed using Student's *t* tests. Values represent the means ± SE of three independent samples. Single asterisks indicate $P < 0.05$; double asterisks indicate $P < 0.01$.

effective reductions in transcript levels of the fungal target genes (Fig. 2B). Values are expressed relative to the endogenous *Pst* reference gene *EF-1* (*PsEF-1*), with the empty vector (BSMV:γ) set to 1 (Yin et al., 2011). To demonstrate the specificity of VIGS against *PsKPP4*, *PsFUZ7*, and *PsKPP6*, the expression of their closest homologs at 2 dpi was also examined (Supplemental Fig. S1; Supplemental Table S3).

Microscopic analyses revealed that initial haustorium formation and elongation of secondary hyphae are both reduced in BMSV:*PsFUZ7*-1as and BMSV:*PsFUZ7*-2as treated plants (Fig. 3). *PsFUZ7*-2as-silenced plants exhibit a more pronounced inhibition of haustorium formation and mycelial extension with decreased hyphal length and reduced size of infection areas compared to other silencing constructs. As a result, fewer uredia were produced in plants carrying BMSV:*PsFUZ7*-2as (Fig. 2C). This result indicates that *PsFUZ7* plays an important role in mycelial growth and development that eventually leads to a significant inhibition of uredia generation and virulence of *Pst*.

The Function of *Ps*FUZ7 Is Conserved among Phytopathogenic Fungi

PsFUZ7 contains the typical domain structure of MAPKKs, including 12 catalytic kinase subdomains

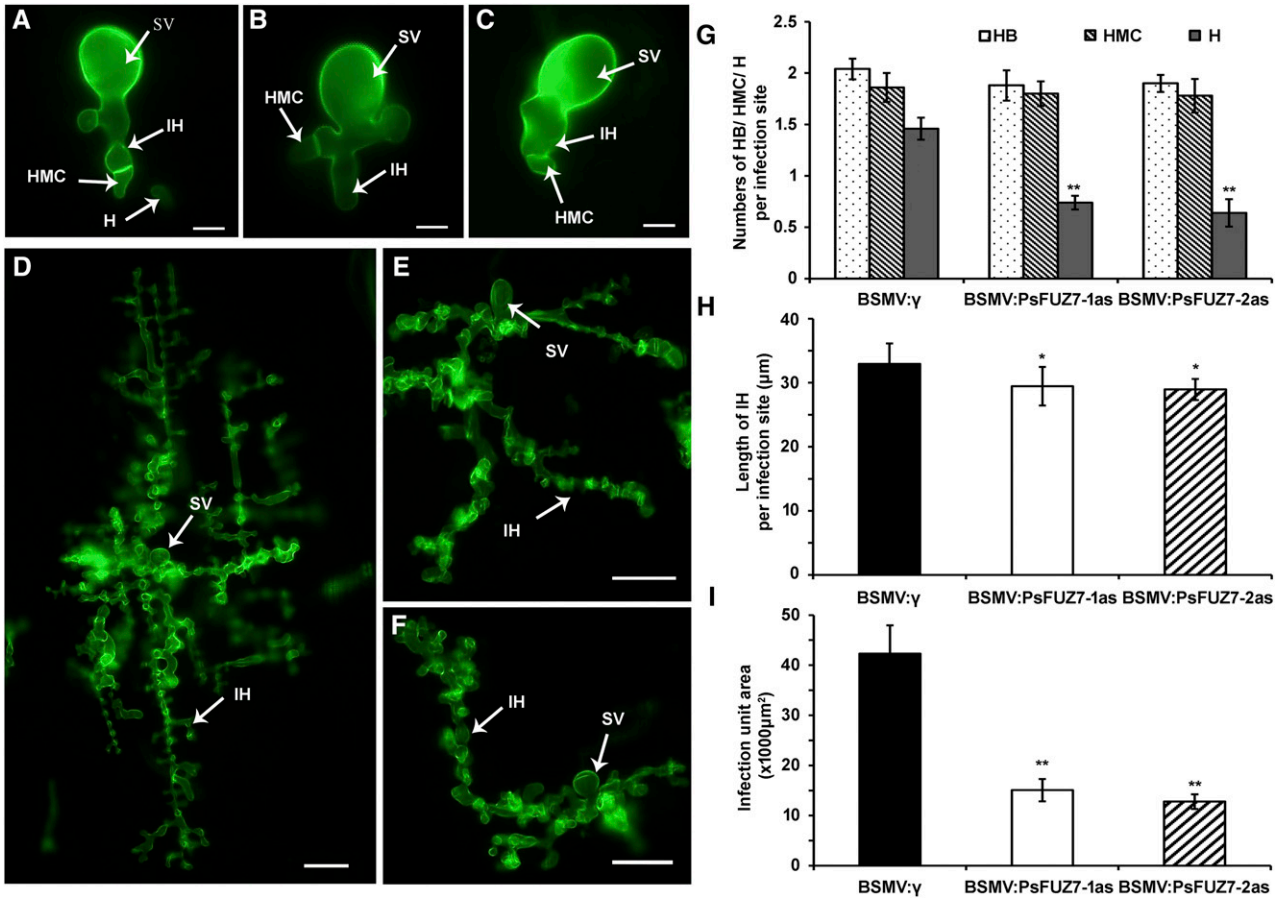

Figure 3. Epifluorescence observation of fungal growth in wheat inoculated with BSMV and infected with CYR32. Leaves inoculated with CYR32 were sampled at 48 and 120 hpi and examined under an epifluorescence microscope after staining with wheat germ agglutinin conjugated to Alexa-488 (Invitrogen). Treatments include BSMV:γ (A), BSMV:*PsFUZ7*-1as (B), BSMV:*PsFUZ7*-2as inoculated with CYR32 at 48 hpi (C; bars = 10 μm), BSMV:γ (D), BSMV:*PsFUZ7*-1as (E), and BSMV:*PsFUZ7*-2as inoculated with CYR32 at 120 hpi (F; bars = 50 μm). G, Average number of H, HB, and HMC in wheat inoculated with BSMV constructs and infected with CYR32 at 48 hpi. H, Average length of IH measured from their origin at the SV to the tip of the hypha in wheat inoculated with BSMV constructs and infected with CYR32 at 48 hpi. I, Infection area per infection site in wheat inoculated with BSMV and infected with CYR32 at 120 hpi. Differences in G to I were assessed using Student's *t* tests. Values represent the means ± standard errors of three independent samples. Single asterisks indicate $P < 0.05$, and double asterisks indicate $P < 0.01$. SV, Substomatal vesicle; HMC, haustorial mother cell; IH, infection hypha; HB, hyphal branches; H, haustorium or haustoria.

(Hamal et al., 1999), two putative phosphorylation sites, an activation loop (S/TXXXS/T) as the putative target of an upstream MAPKKK, and a DEJL motif (K/R-K/R-K/R-X (1-5)-L/I-X-L/I) at the N terminus, which is known to function as a MAPK docking site (Supplemental Fig. S2; Chen et al., 2012). Sequence alignments indicate that *PsFUZ7* shares 70, 82, and 84% sequence identity with orthologs from *Magnaporthe oryzae*, *Puccinia triticina*, and *Puccinia graminis* f. sp. *tritici*, respectively. Consistent with this high similarity, *PsFUZ7* partially complements the *M. oryzae mst7* mutant in appressorium formation and plant infection (Supplemental Fig. S3). Overexpression of *PsFUZ7* in fission yeast results in morphological changes and an increased sensitivity to environmental stresses (Supplemental Fig. S4). In accordance with these in vivo data, in vitro assays revealed that stripe rust urediospores treated with the kinase inhibitor U0126 germinate at a lower rate and produce a higher frequency of abnormally differentiated and clearly distorted germ tubes or spherical structures along the mycelial apex at 3 and 6 h post-treatment (Supplemental Fig. S5). Overall, these results strengthen the view that *PsFUZ7* may have important roles in pathogenesis.

RNAi Constructs in Transgenic Wheat Plants Detected by Southern Blot and PCR

To test whether the stable expression of *PsFUZ7* silencing constructs can confer resistance to *Pst*, the selected, most effective RNAi construct, a 759-bp cassette containing an inverted repeat derived from *PsFUZ7*-2as, was introduced into vector pAHC25, and transformed

into *T. aestivum* cv Xinong1376 (XN1376) by particle bombardment (Supplemental Fig. S6A). The *PsFUZ7*-RNAi construct in transgenic wheat plants was detected by PCR (Supplemental Fig. S6B), and the stable integration of RNAi constructs into the wheat genome was verified by Southern blot with specific probes (Supplemental Fig. S6C). No consecutive 21- to 24-nucleotide sequences were found in wheat and/or other plant or fungal species for *PsFUZ7* (Supplemental Table S4). To identify potential off-target sites, BLASTN was performed using the target sequence. Among all putative off-targets examined, 12 sequences were detected in wheat and *Pst* at one or more locus with a 1- to 3-bp mismatch, respectively (Supplemental Fig. S7; Supplemental Table S2). No significant down-regulation was found in the potential putative off-target genes (Supplemental Figs. S7 and S8). Transgenic wheat lines that contained RNAi constructs, displayed normal morphology, and set viable seeds, were assayed for resistance against *Pst*.

Two T_3 Transgenic Wheat Lines Confer Strong Resistance to *Pst*

Two independent transgenic lines, L65 and L91, which were highly effective in restricting the spread of *Pst*, were selected in T_3 generations and examined at 16 dpi (Fig. 4A). To verify whether this phenotype is caused by the expression and processing of siRNA, northern-blot analysis was performed with RNA extracted from 14-d-old seedlings of the T_3 transgenic lines, using the same specific probes as those used for southern-blot analyses. A single band with the expected size of approximately 21 nucleotides is present in transgenic lines L65 and L91, whereas no signal can be detected in control plants, documenting the presence of *PsFUZ7* siRNAs in the transgenic lines (Fig. 4B). To further confirm that the expression of siRNA in wheat is able to silence *PsFUZ7*, qRT-PCR was performed to analyze transcript abundance of *PsFUZ7* in *Pst*-infected transgenic lines at 3, 10, and 16 dpi. *PsFUZ7* transcripts in L65 were reduced by 42.2, 48.3, and 49.3% compared to control lines at 3, 10, and 16 dpi, respectively. Similarly, *PsFUZ7* transcripts were reduced by 41.7, 69.9, and 74.8% in L91 (Fig. 4C). According to the McNeal's uniform scale system (McNeal et al., 1971) the host response class of transgenic lines L65 and L91 ranged from 1 to 3, indicating high or medium resistance to *Pst*. By contrast, the response of control lines was in the 6 to 7 class, which along with abundant sporulation and few necrotic/chlorotic stripes indicates susceptibility

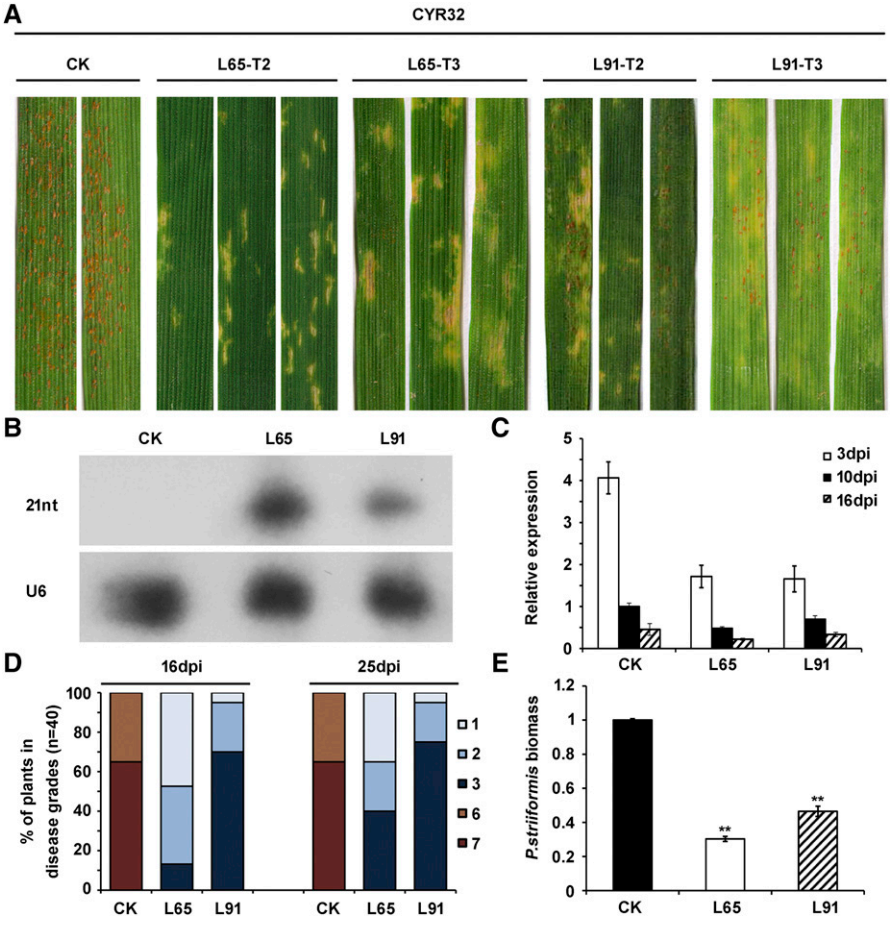

Figure 4. Transgenic wheat lines L65 and L91 producing fungal gene-derived siRNAs induce silencing of the target mRNA and confer resistance to *Pst* infection. A, Phenotypes of transgenic lines L65, L91, and control in T2 and T_3 generations. The second leaves of seedlings were inoculated with urediospores of CYR32 and photographed at 16 dpi with *Pst* in each generation. Control is the transgenic lines carrying empty vector; L65 and L91 are the transgenic lines carrying RNAi constructs. B, Northern-blot analysis of siRNA isolated from T_3 transgenic wheat lines detected with specific probe derived from the *PsFUZ7* fragment. U6 is the small nuclear RNA as a loading control. C, Relative expression of *PsFUZ7* at 3, 10, and 16 dpi with CYR32 of T_3 transgenic wheat lines L65, L91, and control. Data were normalized to *PsEF-1*, and the CK-10 d control was set to 1. D, Host response and infection types in T_3 transgenic wheat lines L65, L91, and control assessed at 16 and 25 dpi with CYR32. E, Fungal biomass measured using real-time PCR of total DNA extracted from wheat leaves infected with CYR32 at 16 dpi. Ratio of total fungal DNA to total wheat DNA was assessed using the wheat gene *TaEF-1* and the *Pst* gene *PsEF-1*. Differences were assessed using Student's *t* tests. Values represent the means ± SE of three independent samples. Double asterisks indicate $P < 0.01$. CK, Control.

to *Pst* (Fig. 4D). Biomass analyses showed that both transgenic lines exhibit significant reductions in fungal biomass ($P < 0.01$) of 68% to 71% and 50% to 57%, respectively, at 16 dpi with *Pst* (Fig. 4E). In addition, compared with control plants, transcript levels of some MAPK signal pathway-related genes (Fig. 5A) are reduced in *Pst*-infected transgenic lines L65 and L91, whereas some plant defense-related genes are up-regulated (Fig. 5B). These results demonstrate that transgenic wheat lines carrying RNAi constructs can produce and process siRNA molecules that efficiently down-regulate *PsFUZ7* in *Pst*, and also affect the expression of some related genes in *Pst* and wheat.

Pst Development and Growth Is Severely Suppressed in Transgenic Wheat Lines Carrying *PsFUZ7* RNAi Constructs

To investigate *Pst* development in transgenic wheat lines L65 and L91, fungal structures were stained with wheat germ agglutinin for microscopic observation. *Pst* in transgenic lines L65 and L91 exhibits poorly developed hyphae with minimal haustorium formation, whereas a widespread hyphal network with numerous haustoria in mesophyll cells is observed in control plants at 10 dpi with CYR32 (Fig. 6, A–C). Notably, large areas of hypersensitive cell death are induced in transgenic lines L65 and L91 (Fig. 6, A and D). The observed restriction of fungal development within siRNA-producing host tissue is consistent with the measured reduction of fungal biomass and uredia formation.

To further visualize mycelial growth in *Pst*-infected wheat tissue, transmission electron microscopy was used to examine fungal morphology and wheat cells (Fig. 6E). Disassembly of the nuclear envelope and shrinkage of protoplasts is observed in *Pst* cells during colonization of the tissue of transgenic plants L65 and L91 (Fig. 6E). In addition, plant plasma membranes were ruptured where they contacted *Pst* hyphae. By contrast, both fungal and host cells developed normally in control lines (Fig. 6E). These results indicate that RNAi molecules stably expressed in transgenic wheat plants are able to confer genetically stable resistance to rust fungi by targeting fungal *PsFUZ7* transcripts, resulting in the suppression of *Pst* growth.

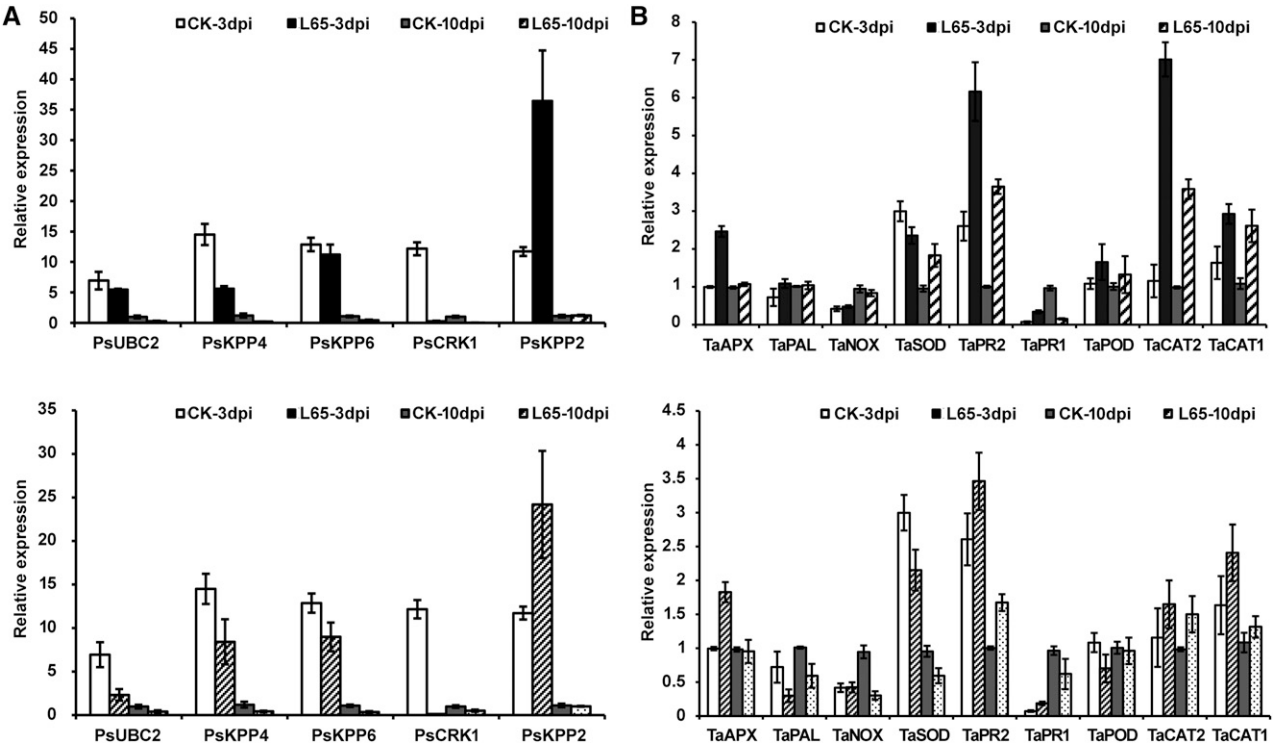

Figure 5. Transcript profiles of genes involved in the MAPK pathway in *Pst* and defense-related genes in transgenic wheat plants L65 and L91. A, Transcript abundance of MAPK pathway-related genes in *Pst* decreases except for *PsKPP2*. Wheat leaves were sampled at 3 and 10 dpi with *Pst*. Data were normalized to the *PsEF-1* expression level, and the CK-10d control was set to 1. B, Transcript abundance of pathogenesis-related proteins or defense-related genes increase in transgenic wheat plants L65 and L91 at 3 and 10 dpi. The data were normalized to the *TaEF-1* expression level, and the CK-10d control was set to 1. Values represent the means ± SE of three independent samples. *PsKPP4*, MAP kinase kinase kinase; *PsFUZ7*, MAP kinase kinase; *PsKPP2*, *PsKPP6*, and *PsCRK1*, MAP kinase; *TaPR1*, pathogenesis-related protein 1; *TaPR2*, β-1,3-glucanase; *TaPAL*, Phe ammonia lyase; *TaAPX*, ascorbate peroxidase; *TaNOX*, NADPH oxidase; *TaSOD*, superoxide dismutase; *TaPOD*, peroxidase; *TaCAT2*, catalase 2; *TaCAT1*, catalase 1.

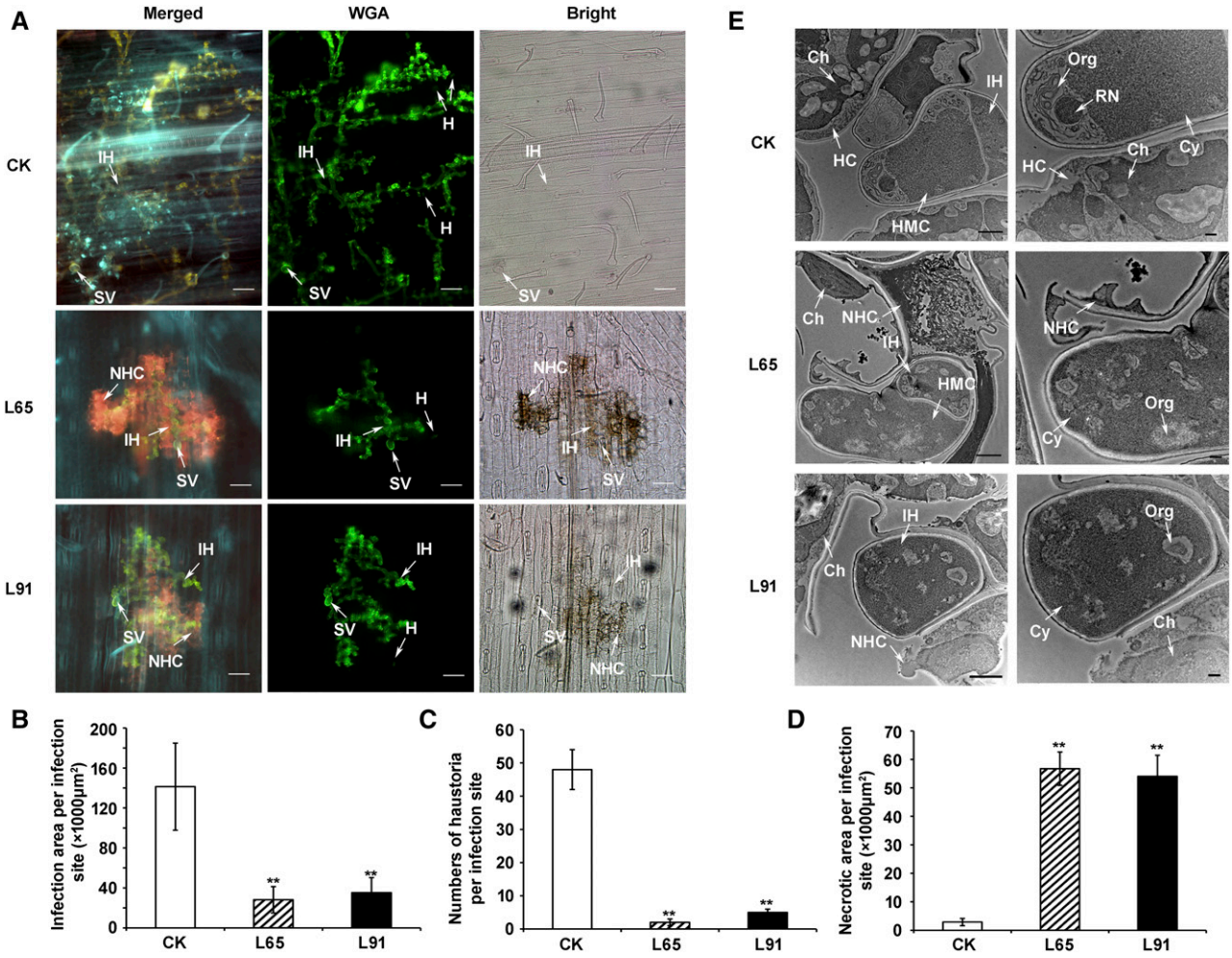

Figure 6. Microscopy visualization of the in host-induced gene-silencing effect targeting *PsFUZ7* on colonization of wheat leaf tissue by *Pst*. A, Cytological observation of rust interaction with wheat by epifluorescence microscopy. Leaves inoculated with CYR32 were sampled at 10 dpi. Bars = 50 μm. B, Infection area per infection site is reduced in the transgenic lines L65 and L91 infected with CYR32 compared with control at 10 dpi. C, The formation of haustoria in lines L65 and L91 is inhibited after inoculation with CYR32 compared with control at 10 dpi. D, The necrotic area of plants from lines L65 and L91 is increased compared with control at 10 dpi with CYR32. E, Cytological observations of *Pst* CYR32 and wheat by transmission electron microscopy at 10 dpi. Left bars = 2 μm; right bars = 500 nm. Differences in D and E were assessed using Student's *t* tests. Values represent the means ± SE of three independent samples. Double asterisks indicate $P < 0.01$. Ch, Chloroplast; CK, control; Cy, cytoplasm; H, haustorium; HC, host cell; HMC, haustorial mother cell; IH, infection hypha; NHC, necrotic host cell; Org, organelle; RN, rust nucleus; SV, substomatal vesicle.

DISCUSSION

Currently, the most effective strategy to control stripe rust disease is the application of fungicides. However, fungicide residues on food products remain a threat to human health (Singh et al., 2015). Traditional plant breeding to improve crop traits is another effective strategy, but is time-consuming and labor-intensive (Saurabh et al., 2014). During the last two decades, research efforts have focused on strategies to convert to biotechnological approaches for crop improvement. The emergence of RNAi, which can be employed to manipulate gene expression to improve quality traits in crops, offers potential promise (Baulcombe, 2004; Saurabh et al., 2014). However, it remained unclear whether *Pst* has a functional silencing system that can be induced in transgenic wheat carrying RNAi constructs. Our approach was to determine whether the expression of RNAi molecules derived from the MAPK kinase gene *PsFUZ7* in transgenic wheat could confer genetically stable resistance to rust pathogens of wheat. *PsFUZ7* was selected as the target gene for silencing because it is expressed at high levels during penetration and parasitic stages of the *Pst*-wheat interaction and showed the most positive phenotype in virus-induced transient silencing assays compared with two other kinases (Fig. 1). In the fungal kingdom, MAPK kinases are evolutionarily conserved proteins that function as key signal transduction components regulating a series

of cellular processes (Hamel et al., 2012). In the functional screening of candidate genes for the generation of efficient RNAi sequences, supplementary assays confirmed that the *PsFUZ7* is functionally conserved with MAPKKs from other fungi and participates in development and morphogenesis critical for virulence of *Pst*. Off-target effects, resulting in the knockdown of other transcripts with limited similarity to siRNA, often occur during the application of RNAi in plants and humans (Birmingham et al., 2006; de Souza, 2014). In our study, no off-target effects were detected, indicating that the *PsFUZ7* fragment selected to generate RNAi constructs could be an ideal target for control of *Pst* via RNAi (Supplemental Table S3).

This study is devoted to illustrating an efficient alternative approach to conventional breeding and fungicide treatment for fungal disease control. As expected, transgenic lines carrying *PsFUZ7* RNAi constructs exhibit strong and genetically stable resistance to *Pst* in T_3 generations (Fig. 4A). Generally, the T_3 generation is considered the initial true transgenic line in hexaploid wheat (Cheng et al., 2015a). Histological observations revealed differential hyphal growth in transgenic lines carrying *PsFUZ7* RNAi constructs compared to the control lines (Fig. 6). Previous studies demonstrated the efficient transport of siRNA molecules from transgenic plant cells to the colonizing pathogen (Nowara et al., 2010; Koch et al., 2013), and that the transported siRNAs interfere with the target gene, affecting fungal growth through an amplification of RNAi molecules and resulting in a resistance response (Panwar et al., 2013; Cheng et al., 2015a). The suppression of *Pst* growth in our study correlates with the production of siRNAs corresponding to the targeted *PsFUZ7* sequences (Fig. 4B), as well as a significant reduction of *PsFUZ7* transcripts and fungal biomass (Fig. 4, C and E).

To explore the basis for the induction of necrosis in plant cells, a schematic presentation for potential processes triggered by silencing *PsFUZ7* via the expression of siRNA in transgenic wheat is presented (Fig. 7). In the plant immunity system, two main phases, pathogen-associated molecular patterns (PAMPs) triggered immunity (PTI) and effector-triggered immunity (ETI), are well known (Jones and Dangl, 2006; Boller and Felix, 2009; Tsuda and Katagiri, 2010). Cell death induced in transgenic wheat lines is in accordance with a hypersensitive response that is expressed in pathogen-specific ETI (Jones and Dangl, 2006; Thomma et al., 2011). In *U. maydis*, the kinase CRK1 downstream of the MAPK cascade negatively regulates transcription and secretion of some effector proteins (Bielska et al., 2014). In our study, we verified the severe down-regulation of *PsCRK1* transcripts (Fig. 5) and the interaction between *PsFUZ7* and *PsCRK1* via the yeast-two hybrid assay (Supplemental Fig. S9). Considering these results, we propose that the expression of the siRNA target *PsFUZ7* influences effectors in *Pst* and triggers ETI in transgenic XN1376 wheat (Fig. 7). In addition, many features associated with fungal pathogenesis are dependent on signaling through MAPK cascades, including the biosynthesis, export, and secretion of

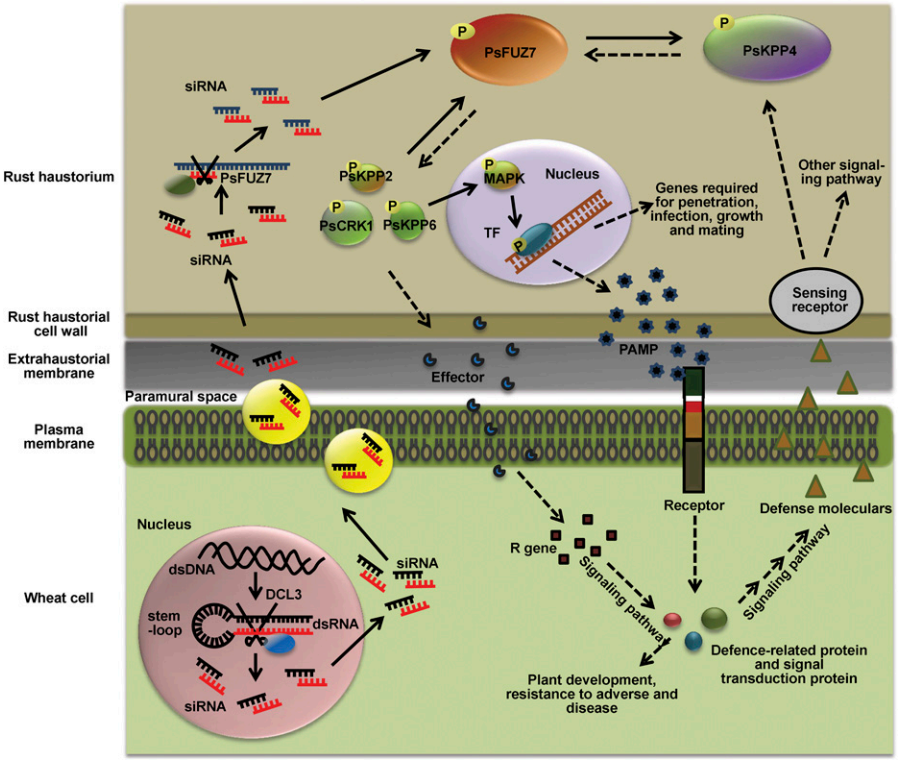

Figure 7. Schematic presentation of possible molecular dialogues between transgenic lines carrying RNAi constructs and colonizing *Pst*. Fungal dsRNA, produced inside transgenic wheat cells, is cleaved by the plant silencing machinery using endonuclease-type DICER enzymes into small silencing molecules (siRNAs). These siRNAs are trapped by a complex of proteins, and transported to the paramural space. After passing the haustorial cell wall, the silencing molecules trigger RNAi of their mRNA targets, and may act as primers leading to the activation of systemic silencing signals, thus inducing the immunity system of transgenic wheat by mechanisms including ETI and PTI.

different factors (Hamel et al., 2012). HIGS of *PsFUZ7* may impact biosynthesis or secretion of *Pst* components that may function as PAMPs in PTI (Chisholm et al., 2006).

Our study has confirmed that the expression of siRNA derived from a *Pst* pathogenicity gene in wheat is an effective strategy to control rust disease. This approach provides a huge reservoir, to our knowledge, of novel resources to enhance resistance to abiotic and biotic stress by the production of transgenic crops that are environmentally friendly.

MATERIALS AND METHODS

Fungi, Plants, and Culture Conditions

Chinese Yellow Rust isolate 32 (CYR32), which is a predominant race in China (Wan et al., 2007), was used throughout this study. Wheat (*Triticum aestivum* cv Suwon11 [Su11]) that is susceptible to CYR32 was used in qRT-PCR and VIGS assays. Plant cultivation and inoculation with *Pst* were performed as described previously (Kang et al., 2002). XN1376, susceptible to CYR32 at the seedling stage, was grown in an experimental field of Northwest A&F University and used for transgenic wheat cultivars.

VIGS and RNAi Vector Construction

Two *PsFUZ7* fragments were used in BSMV-induced gene-silencing experiments (Supplemental Table S2). *PsFUZ7*-1as contains 218 bp of the coding sequence from the 5′ region, whereas *PsFUZ7*-2as encompasses a 300-bp coding sequence in the 3′ UTR. The two fragments were cloned into BSMV as previously described (Holzberg et al., 2002). The hpRNA cassette contains the maize (*Zea mays*) *alcohol dehydrogenase 1* (*adh1*) gene as an intron flanked by the 300-bp fragment of *PsFUZ7* in sense and antisense orientations. The expression cassette treated with *Sma*I and *Sac*I was cloned into the binary vector pAHC25 using the same restriction sites (Christensen et al., 1992; Vasil et al., 1993). The *bar* gene in the T-DNA of the vector as selection gene is driven by the maize ubiquitin promoter, and the hpRNA cassette is also under control of the Ubi promoter and terminated by the NOS terminator. The resulting vectors were pAHC25-hp*PsFUZ7* for silencing *PsFUZ7*, and the empty vector pAHC25 containing only the *bar* gene without a silencing cassette.

Total DNA, RNA Extraction, PCR, and qRT-PCR

Genomic DNA was extracted by the CTAB method (Porebski et al., 1997). RNA was isolated with TRIZOL following the manufacturer's instructions (Invitrogen) and transcribed into cDNA, also following the manufacturer's directions (Promega). In each transgenic generation, genomic DNA from leaves of transgenic wheat and control plants were identified by PCR with two pairs of specific primers (TFUZ-F/R and Bar-F/R; Supplemental Table S2) to detect the presence of the sense-intron-antisense cassette in transgenic plants and the *bar* gene. To measure fungal biomass, relative quantification of the single-copy target genes in *PsEF-1* and *TaEF-1* (elongation factor-1) was carried out (Panwar et al., 2013). Total genomic DNA of the wheat cultivar XN1376 or the *Pst* isolate CYR32 was used to prepare standard curves derived from at least six serial dilutions for each. The correlation coefficients for the analysis of the dilution curves were above 0.99. The relative quantities of the PCR products of *PsEF-1* and *TaEF-1* in mixed/infected samples were calculated using the gene-specific standard curves to quantify the *Pst* and wheat genomic DNA, respectively.

To measure the transcript levels of *PsFUZ7* by qRT-PCR, urediospores and in vivo germ tubes of CYR32, plant tissue of Su11 infected with CYR32 at 6, 12, 18, 24, 36, 48, 72, 120, 168, and 216 h postinoculation (hpi) and urediospores were sampled. To analyze VIGS efficiency, qRT-PCR was carried out 48 and 168 hpi with the CYR32 isolate. For transgenic efficiency assay, total transgenic RNA for quantitative real-time PCR was extracted from the second leaves of wheat at 3, 10, and 16 dpi with the CYR32 isolate. All qRT-PCR was performed in a 20-μL reaction mixture containing LightCycler SYBR Green I Master Mix (Roche), 10 pmol each of the forward and reverse gene-specific primers (Supplemental Table S2), and 2 μL of diluted cDNA (1:5) that was reverse transcribed. PCR was run in a LightCycler 480II (Roche) under the conditions previously described (Cheng et al., 2015b). Each sample was analyzed in three biological replications, and each PCR analysis included three technical repeats. The data were normalized to the *PsEF-1* expression level.

BSMV-Mediated Gene Silencing

Capped in vitro transcripts were prepared from linearized plasmids containing the tripartite BSMV genome (Petty et al., 1990) using the RiboMAX Large-Scale RNA Production System-T7 and the Ribom7G Cap Analog (both by Promega), according to the manufacturer's instructions. PsFUZ7-1as and PsFUZ7-2as were used to inoculate wheat seedlings, whereas BSMV:TaPDS (TaPDS is the wheat phytoene desaturase gene) and BSMV:γ were used as controls for the BSMV infection. Mock plants were inoculated with 1× FES buffer as the negative control. Wheat seedlings with three leaves were used for inoculation with BSMV, and BSMV-infected wheat plants were kept in a growth chamber at 23 ± 2°C. The fourth leaves were further inoculated with fresh CYR32 urediospores at 10 d after virus inoculation, and the plants were then maintained at 16 ± 2°C (Wang et al., 2007). The phenotypes of the fourth leaves were recorded and photographed at 14 d after inoculation with *Pst*. The number of uredia was counting a 1 cm^2 area at 14 dpi with *Pst* from at least five randomly treated plants.

Cytological Observation of Fungal Growth and Host Responses

Leaf segments (1.5 cm long) were cut from inoculated leaves, fixed, and decolorized in ethanol/trichloromethane (3:1 v/v) containing 0.15% (w/v) trichloroacetic acid for 3 d to 5 d, and then treated as previously described (Cheng et al., 2015b). To obtain high-quality images of *Pst* infection structures in wheat leaves, wheat germ agglutinin conjugated to Alexa-488 (Invitrogen) was used as described (Ayliffe et al., 2011). Stained tissue was examined under blue light excitation (excitation wavelength 450 nm to 480 nm, emission wavelength 515 nm). Necrotic area was observed via the autofluorescence of the mesophyll cells in infected leaves using epifluorescence microscopy (excitation filter, 485 nm; dichromic mirror, 510 nm; barrier filter, 520 nm). Infection sites (30 to 50) from three leaves were examined to record the number of haustorial mother cells, haustoria, hyphal branches, hyphal length, and infection areas of hyphae or necrotic areas of host cells in infected wheat per infection unit. The experiments were conducted in a completely randomized block design with three replications. The presence of a substomatal vesicle was defined as an established infection unit. Hyphal length of *Pst* was measured from the substomatal vesicle to the apex of the longest infection hypha. All microscopic observations were conducted with a model BX-51 microscope (Olympus).

To observe the ultrastructure of the fungus, wheat leaves bearing uredia were cut into 0.5 × 0.5 cm pieces, immersed in 4% glutaraldehyde in 0.2 M P buffer, pH 6.8, and fixed at 4°C overnight (Zhan et al., 2014). Fixed leaf samples were washed four times with P buffer for 15 min each. Thereafter, samples were successively dehydrated for 30 min each in 30, 50, 70, 80, and 90% ethanol, and finally three times in 100% ethanol. The dehydrated samples were treated with isoamyl acetate twice for 20 min each. After drying in a CO_2 vacuum, the samples were sputter-coated with gold in an E-1045 (Hitachi) and then examined with an S-4800 SEM (Hitachi).

Plant Transformation

Immature embryos were isolated from spikes of XN1376 at 13 to 14 d postanthesis in Yangling, Shaanxi. The isolated wheat embryos were cultured on SD_2 medium in the dark for 7 to 10 d for calli induction (Li et al., 2008). Then the calli were moved to SD_2 medium added with 0.2 mol/L mannitol and 0.2 mol/L sorbitol. After 4 to 6 h, the calli were bombarded with 1-μm gold particles coated with 1.5 μg of recombinant pAHC25 DNA using a PDS-1000 He biolistic gun (Bio-Rad) at the pressure of 1,100 p.s.i. (Vasil et al., 1993; Li et al., 2008). The bombarded calli were transferred onto the osmotic pressure medium described above for 16 to 18 h. Regeneration and selection were carried out in the corresponding medium in the presence of 3 mg/L to 5 mg/L bialaphos for the next few weeks, and the surviving plantlets with strong roots and shoots were planted in a greenhouse in pots filled with soil (Cheng et al., 2015a).

Northern Blot

Approximately 30 μg of total RNA was subjected to electrophoresis on a denaturing 19% polyacrylamide gel, transferred to Nytran Super Charge Nylon Membranes (Schleicher und Schuell MicroScience) and cross-linked using a Stratagene UV Cross Linker. The membranes were prehybridized with PerfectHyb (Sigma-Aldrich) and hybridized with the P^{32}-labeled DNA probes overnight in PerfectHyb buffer (Sigma-Aldrich). The membranes were autoradiographed on X-OMAT BT film (Carestream Health) after rinsing with washing buffer. U6 was used as a loading control. The probe sequences are listed in Supplemental Table S2.

Accession Numbers

Sequence data from this article can be found in the GenBank/EMBL data libraries under the following accession numbers: PsKPP4 (KNE89636.1), PsFUZ7(GQ979632.1), PsKPP6 (KNE97907.1), PsKPP2 (KNE99344.1), and PsCRK1 (KNE97720.1).

Supplemental Data

The following supplemental materials are available.

Supplemental Figure S1. Relative transcript levels of *PsKPP4*, *PsFUZ7*, and *PsKPP6* homologs in respective knockdown plants inoculated with CYR32 at 2 dpi.

Supplemental Figure S2. Multiple sequence alignment of *FUZ7* orthologs.

Supplemental Figure S3. Complementation of the *mst7* mutant of *M. oryzae* with *PsFUZ7*.

Supplemental Figure S4. Overexpression assay of *PsFUZ7* in the fission yeast SP-Q01.

Supplemental Figure S5. Effect of the immunosuppressive inhibitor U0126 on germination of *Pst*.

Supplemental Figure S6. Structure of the pAHC25-*PsFUZ7* RNAi construct and molecular identification in transgenic plants.

Supplemental Figure S7. Transcript abundance of putative off-target in *Pst* after L65, L91, and CK inoculated with CYR32 at 10 dpi.

Supplemental Figure S8. Transcript abundance of putative off-target in wheat after L65, L91, and CK inoculated with CYR32 at 10 dpi.

Supplemental Figure S9. Y2H assay using MAPK cascade genes.

Supplemental Table S1. MAPK orthologs identified in *Pst*.

Supplemental Table S2. Primers used in this study.

Supplemental Table S3. Homologs of PsKPP4, PsFUZ7, and PsKPP6 in *Pst*.

Supplemental Table S4. Prediction of *PsFUZ7* off-target transcripts.

ACKNOWLEDGMENTS

We thank Professor Jiankang Zhu (Shanghai Center for Plant Stress Biology, SIBS, CAS, China) for providing technical support on southern- and northern-blot analysis and Professor Larry Dunkle (USDA-Agricultural Research Service at Purdue University) for critical reading of the manuscript.

Received October 3, 2017; accepted October 20, 2017; published October 25, 2017.

LITERATURE CITED

Ayliffe M, Devilla R, Mago R, White R, Talbot M, Pryor A, Leung H (2011) Nonhost resistance of rice to rust pathogens. Mol Plant Microbe Interact **24:** 1143–1155

Bartel DP (2004) MicroRNAs: genomics, biogenesis, mechanism, and function. Cell **116:** 281–297

Baulcombe D (2004) RNA silencing in plants. Nature **431:** 356–363

Baum JA, Bogaert T, Clinton W, Heck GR, Feldmann P, Ilagan O, Johnson S, Plaetinck G, Munyikwa T, Pleau M, Vaughn T, Roberts J (2007) Control of coleopteran insect pests through RNA interference. Nat Biotechnol **25:** 1322–1326

Bielska E, Higuchi Y, Schuster M, Steinberg N, Kilaru S, Talbot NJ, Steinberg G (2014) Long-distance endosome trafficking drives fungal effector production during plant infection. Nat Commun **5:** 5097

Birmingham A, Anderson EM, Reynolds A, Ilsley-Tyree D, Leake D, Fedorov Y, Baskerville S, Maksimova E, Robinson K, Karpilow J, Marshall WS, Khvorova A (2006) 3′ UTR seed matches, but not overall identity, are associated with RNAi off-targets. Nat Methods **3:** 199–204

Boller T, Felix G (2009) A renaissance of elicitors: perception of microbe-associated molecular patterns and danger signals by pattern-recognition receptors. Annu Rev Plant Biol **60:** 379–406

Chen T, Zhu H, Ke D, Cai K, Wang C, Gou H, Hong Z, Zhang Z (2012) A MAP kinase interacts with SymRK and regulates nodule organogenesis in *Lotus japonicus*. Plant Cell **24:** 823–838

Chen WQ, Wu LR, Liu TG, Xu SC, Jin SL, Peng YL, Wang BT (2009) Race dynamics, diversity, and virulence evolution in *Puccinia striiformis* f. sp. *tritici*, the causal agent of wheat stripe rust in China from 2003 to 2007. Plant Dis **93:** 1093–1101

Chen XM (2014) Integration of cultivar resistance and fungicide application for control of wheat stripe rust. Can J Plant Pathol **36:** 311–326

Cheng W, Song XS, Li HP, Cao LH, Sun K, Qiu XL, Xu YB, Yang P, Huang T, Zhang JB, Qu B, Liao YC (2015a) Host-induced gene silencing of an essential chitin synthase gene confers durable resistance to *Fusarium* head blight and seedling blight in wheat. Plant Biotechnol J **13:** 1335–1345

Cheng Y, Wang X, Yao J, Voegele RT, Zhang Y, Wang W, Huang L, Kang Z (2015b) Characterization of protein kinase PsSRPKL, a novel pathogenicity factor in the wheat stripe rust fungus. Environ Microbiol **17:** 2601–2617

Chisholm ST, Coaker G, Day B, Staskawicz BJ (2006) Host-microbe interactions: shaping the evolution of the plant immune response. Cell **124:** 803–814

Christensen AH, Sharrock RA, Quail PH (1992) Maize polyubiquitin genes: structure, thermal perturbation of expression and transcript splicing, and promoter activity following transfer to protoplasts by electroporation. Plant Mol Biol **18:** 675–689

de Souza N (2014) Off-targets in RNAi screens. Nat Methods **11:** 480

Fagard M, Boutet S, Morel JB, Bellini C, Vaucheret H (2000) AGO1, QDE-2, and RDE-1 are related proteins required for post-transcriptional gene silencing in plants, quelling in fungi, and RNA interference in animals. Proc Natl Acad Sci USA **97:** 11650–11654

Fu Y, Duan X, Tang C, Li X, Voegele RT, Wang X, Wei G, Kang Z (2014) TaADF7, an actin-depolymerizing factor, contributes to wheat resistance against *Puccinia striiformis* f. sp. *tritici*. Plant J **78:** 16–30

Ghag SB, Shekhawat UK, Ganapathi TR (2014) Host-induced post-transcriptional hairpin RNA-mediated gene silencing of vital fungal genes confers efficient resistance against *Fusarium* wilt in banana. Plant Biotechnol J **12:** 541–553

Ghildiyal M, Zamore PD (2009) Small silencing RNAs: an expanding universe. Nat Rev Genet **10:** 94–108

Hamal A, Jouannic S, Leprince AS, Kreis M, Henry Y (1999) Molecular characterisation and expression of an *Arabidopsis thaliana* L. MAP kinase cDNA, *AtMAP2Kα*. Plant Sci **140:** 41–52

Hamel LP, Nicole MC, Duplessis S, Ellis BE (2012) Mitogen-activated protein kinase signaling in plant-interacting fungi: distinct messages from conserved messengers. Plant Cell **24:** 1327–1351

Holzberg S, Brosio P, Gross C, Pogue GP (2002) Barley stripe mosaic virus-induced gene silencing in a monocot plant. Plant J **30:** 315–327

Huang G, Allen R, Davis EL, Baum TJ, Hussey RS (2006) Engineering broad root-knot resistance in transgenic plants by RNAi silencing of a conserved and essential root-knot nematode parasitism gene. Proc Natl Acad Sci USA **103:** 14302–14306

Ishii H (2006) Impact of fungicide resistance in plant pathogens on crop disease control and agricultural environment. Jpn Agric R Res Q **40:** 205–211

Jones JD, Dangl JL (2006) The plant immune system. Nature **444:** 323–329

Kang Z, Huang L, Buchenauer H (2002) Ultrastructural changes and localization of lignin and callose in compatible and incompatible interactions between wheat and *Puccinia striiformis*. J Plant Dis Prot **109:** 25–37

Koch A, Kumar N, Weber L, Keller H, Imani J, Kogel KH (2013) Host-induced gene silencing of cytochrome P450 lanosterol C14α-demethylase-encoding genes confers strong resistance to *Fusarium* species. Proc Natl Acad Sci USA **110:** 19324–19329

Li HP, Zhang JB, Shi RP, Huang T, Fischer R, Liao YC (2008) Engineering *Fusarium* head blight resistance in wheat by expression of a fusion protein containing a *Fusarium*-specific antibody and an antifungal peptide. Mol Plant Microbe Interact **21:** 1242–1248

Liu Q, Paroo Z (2010) Biochemical principles of small RNA pathways. Annu Rev Biochem **79:** 295–319

Mao YB, Cai WJ, Wang JW, Hong GJ, Tao XY, Wang LJ, Huang YP, Chen XY (2007) Silencing a cotton bollworm P450 monooxygenase gene by plant-mediated RNAi impairs larval tolerance of gossypol. Nat Biotechnol **25:** 1307–1313

Mcintosh RA, Wellings CR, Park RF, editors (1995) Wheat Rusts: An Atlas of Resistance Genes. Springer, Dordrecht, The Netherlands

McNeal FH, Konzak CF, Smith EP, Tate WS, Russell TS (1971) A uniform system for recording and processing cereal research data. USDA, Agricultural Research Service Bulletin 34–121, p 42

Nowara D, Gay A, Lacomme C, Shaw J, Ridout C, Douchkov D, Hensel G, Kumlehn J, Schweizer P (2010) HIGS: host-induced gene silencing in the obligate biotrophic fungal pathogen *Blumeria graminis*. Plant Cell **22:** 3130–3141

Panwar V, McCallum B, Bakkeren G (2013) Endogenous silencing of *Puccinia triticina* pathogenicity genes through in planta-expressed sequences leads to the suppression of rust diseases on wheat. Plant J **73:** 521–532

Petty ITD, French R, Jones RW, Jackson AO (1990) Identification of barley stripe mosaic virus genes involved in viral RNA replication and systemic movement. EMBO J **9:** 3453–3457

Porebski S, Bailey LG, Baum BR (1997) Modification of a CTAB DNA extraction protocol for plants containing high polysaccharide and polyphenol components. Plant Mol Biol Report **15:** 8–15

Saurabh S, Vidyarthi AS, Prasad D (2014) RNA interference: concept to reality in crop improvement. Planta **239:** 543–564

Scofield SR, Huang L, Brandt AS, Gill BS (2005) Development of a virus-induced gene-silencing system for hexaploid wheat and its use in functional analysis of the Lr21-mediated leaf rust resistance pathway. Plant Physiol **138:** 2165–2173

Singh RP, Hodson DP, Huerta-Espino J, Jin Y, Bhavani S, Njau P, Herrera-Foessel S, Singh PK, Singh S, Govindan V (2011) The emergence of Ug99 races of the stem rust fungus is a threat to world wheat production. Annu Rev Phytopathol **49:** 465–481

Singh RP, Hodson DP, Jin Y, Lagudah ES, Ayliffe MA, Bhavani S, Rouse MN, Pretorius ZA, Szabo LJ, Huerta-Espino J, Basnet BR, Lan C, et al (2015) Emergence and spread of new races of wheat stem rust fungus: continued threat to food security and prospects of genetic control. Phytopathology **105:** 872–884

Thomma BPHJ, Nürnberger T, Joosten MHAJ (2011) Of PAMPs and effectors: the blurred PTI-ETI dichotomy. Plant Cell **23:** 4–15

Tsuda K, Katagiri F (2010) Comparing signaling mechanisms engaged in pattern-triggered and effector-triggered immunity. Curr Opin Plant Biol **13:** 459–465

van Drogen F, Peter M (2002) MAP kinase cascades: scaffolding signal specificity. Curr Biol **12:** R53–R55

Vasil V, Srivastava V, Castillo AM, Fromm ME, Vasil IK (1993) Rapid production of transgenic wheat plants by direct bombardment of cultured immature embryos. Nat Biotechnol **11:** 1553–1558

Wan AM, Chen XM, He ZH (2007) Wheat stripe rust in China. Crop Pasture Sci **58:** 605–619

Wang CF, Huang LL, Buchenauer H, Han QM, Zhang HC, Kang ZS (2007) Histochemical studies on the accumulation of reactive oxygen species (O_2^- and H_2O_2) in the incompatible and compatible interaction of wheat-*Puccinia striiformis* f. sp. *tritici*. Physiol Mol Plant Pathol **71:** 230–239

Wellings CR (2011) Global status of stripe rust: a review of historical and current threats. Euphytica **179:** 129–141

Yin C, Jurgenson JE, Hulbert SH (2011) Development of a host-induced RNAi system in the wheat stripe rust fungus *Puccinia striiformis* f. sp. *tritici*. Mol Plant Microbe Interact **24:** 554–561

Zhan G, Tian Y, Wang F, Chen X, Guo J, Jiao M, Huang L, Kang Z (2014) A novel fungal hyperparasite of *Puccinia striiformis* f. sp. *tritici*, the causal agent of wheat stripe rust. PLoS One **9:** e111484